ELSEVIER

NeuroImage

www.elsevier.com/locate/ynimg
NeuroImage 23 (2004) 25–34

Cooperation of different neuronal systems during hand sign recognition

Akinori Nakamura,* Burkhard Maess, Thomas R. Knösche, Thomas C. Gunter, Patric Bach, and Angela D. Friederici

Max Planck Institute for Human Cognitive and Brain Sciences, Leipzig, Germany

Received 19 June 2003; revised 9 March 2004; accepted 28 April 2004

Hand signs with symbolic meaning can often be utilized more successfully than words to communicate an intention; however, the underlying brain mechanisms are undefined. The present study using magnetoencephalography (MEG) demonstrates that the primary visual, mirror neuron, social recognition and object recognition systems are involved in hand sign recognition. MEG detected well-orchestrated multiple brain regional electrical activity among these neuronal systems. During the assessment of the meaning of hand signs, the inferior parietal, superior temporal sulcus (STS) and inferior occipitotemporal regions were simultaneously activated. These three regions showed similar time courses in their electrical activity, suggesting that they work together during hand sign recognition by integrating information in the ventral and dorsal pathways through the STS. The results also demonstrated marked right hemispheric predominance, suggesting that hand expression is processed in a manner similar to that in which social signs, such as facial expressions, are processed.

Keywords: Hand signs; Superior temporal sulcus; Magnetoencephalography

Introduction

In our daily communication, we use many "hand signs", which have strong symbolic meanings without verbalization. These symbolic hand signs are a unique type of gesture because they are different from object-oriented actions, can substitute for parts of speech and are independent of any sign language which has linguistic structure (Goldin-Meadow, 1999). Symbolic hand signs can transmit meaning alone (independent of speech) and are therefore classified as emblematic gestures (McNeill, 1992). How do we recognize the hand owner's intention/meaning from the hand signs? Humans have an inherent ability to understand the intentions of others (Carruthers and Smith, 1996). In the case of action perception, it is postulated that an actor's intention can be understood whenever the observed action is mapped onto internal representations of the observer's intentions (Decety and Grezes, 1999; Rizzolatti et al., 2001). Studies in monkeys have found "mirror neurons", which discharge during both observation and execution of actions, in the inferior frontal (Rizzolatti et al., 1996a) and inferior parietal cortices (Fogassi et al., 1998). There are also neurons that respond to goal-directed hand actions in the superior temporal sulcus (STS) (Perrett et al., 1989). Several functional neuroimaging studies have shown that homologous brain regions in humans are activated by action observation, and should have identical neuronal properties as those in monkeys (Decety et al., 1997; Grafton et al., 1996; Iacoboni et al., 1999, 2001; Nishitani and Hari, 2000; Rizzolatti et al., 1996b). Thus, the inferior frontal, inferior parietal and STS regions are considered to play an essential role in action understanding by functioning as the observation–execution matching system (mirror neuron system). On the other hand, an individual's intention is also inferable from other nonverbal cues including facial expression, eye gaze and behavior. Such information is thought to be processed by the social recognition system (Adolphs, 1999; Allison et al., 2000). The STS region is also considered to be a component of the social recognition system because neurons in the STS react to biological motions (Grossman et al., 2000; Oram and Perrett, 1994) that convey social signals, including eye gaze, mouth and lip movements (Calvert et al., 1997; Nishitani and Hari, 2002; Perrett et al., 1985; Puce et al., 1998; Wicker et al., 1998). Besides the STS, the amygdala and orbitofrontal cortex, both of which have reciprocal connections with the STS, and the right somatosensory cortex are involved in the social recognition system (Adolphs, 1999; Allison et al., 2000). In addition, the object recognition system, which involves the ventral occipitotemporal regions (Ungerleider and Haxby, 1994), may also play an important role in analyzing symbolic hand shapes.

As hand signs contain all aspects related to action, social and shape information, one could expect that the three neuronal systems described above should work together during hand sign recognition. If so, the next question is how do these neuronal systems cooperate across anatomically distinct cortical areas? For example, the mirror neuron and object recognition systems are located mainly in the dorsal and ventral pathways, respectively. It is widely accepted that in the ventral and dorsal pathways, different aspects of visual information ("what" and "where/how") are processed in parallel (Livingstone and Hubel, 1988; Ungerleider and Haxby, 1994). Therefore, the

* Corresponding author. Max Planck Institute for Human Cognitive and Brain Sciences, Stephanstrasse 1a, 04103, Leipzig, Germany. Fax: +49-3425-8875-11.

E-mail address: nakamura@cbs.mpg.de (A. Nakamura).

Available online on ScienceDirect (www.sciencedirect.com.)

1053-8119/$ - see front matter © 2004 Elsevier Inc. All right reserved.
doi:10.1016/j.neuroimage.2004.04.034

question appears to involve the so-called "binding problem" (Wolfe and Cave, 1999); that is, how do we finally achieve unified perception/recognition from separately processed information?

To answer these questions, we analyzed the detailed temporal structure of multiple sites of cortical electric activation during hand sign recognition using magnetoencephalography (MEG). We refined MEG data analytic methods to achieve reliable spatiotemporal multiple source estimation. The method, briefly, is as follows: First, individual brain current source density maps (Hämäläinen and Ilmoniemi, 1984, 1994; Knösche et al., 1996) (CSD), reflecting electrical activity in the cortical surface, were calculated. Second, CSD data from each individual were spatially normalized to allow group analyses. Third, a principal component analysis (Dien, 1998; Maess et al., 2002) (PCA) was applied to the CSD data to extract spatiotemporally separable independent factors in the time series. Fourth, using spatial information from the PCA factors, a region of interest (ROI) analysis was applied to the CSD data (PCA-based ROI analysis) to obtain time courses of specific brain regional electrical activity. Using these methods, we show orchestrated multiple brain activity, well structured in time, during understanding the hand signs.

Methods

Subjects

Twenty right-handed German volunteers (mean age 25.3 years, 10 males) participated in the MEG recordings. All participants had natural or corrected visual acuity greater than 25/25, and none of them understood any sign language. Written informed consent was obtained before the experiment. Seven subjects were omitted from data analysis because of low signal to noise ratio in the MEG signal or other technical problems such as large head motions during the measurements. Data sets from 13 subjects were further analyzed. Ten of these subjects participated in an additional reaction time study.

Stimuli and tasks

Before the MEG experiment, a psychological questionnaire was administered to a separate group of participants to select commonly acceptable meaningful and meaningless hand signs. The questionnaire consisted of 66 images of various hand postures. Forty-seven German native speakers rated the meaningfulness of each hand posture subjectively from 1 (definitely meaningless) to 5 (definitely meaningful). Note that the hand postures were recorded independent of speech and were presented in isolation. Finally, we selected 11 meaningful and 11 meaningless hand signs (Fig. 1). Pictures in the two categories were counterbalanced in shape as far as possible. Rating scores for the hand signs are presented in Table 1.

Visual stimuli were 132 digitized gray-scaled photos (400 × 400 pixels) containing 11 meaningful and 11 meaningless hand signs each taken from six adults. Sixty-six different gray-scaled face images (A.M. Martinez and R. Benavente. The AR Face Database. CVC Technical Report #24, June 1998) were also prepared. The experiments were controlled by ERTS-VIPL (Beri-Soft Co., Frankfurt, Germany) and projected onto a screen using a liquid crystal video projector. The visual angle was 13° × 13° and the viewing distance was 70 cm. A small fixation point was placed at the center of the screen.

We measured visual event-related MEG responses to meaningful (HM+) and meaningless (HM−) hand signs while participants assessed the meaningfulness of hand postures (meaning task). We also measured MEG responses to hands (HC) (using the same images as HM+) and faces (FC) during their categorization (categorization task). The meaning task was performed to allow detection of brain regions responsible for meaning/recognition processes, and the categorization task was intended to allow analysis of top-down effects, which are influenced by task-dependent cognitive strategies.

The meaning task, which was to judge the meaningfulness of the hand signs, consisted of following steps: at first, the hand pictures were randomly presented (700 ms) and followed by a blank screen (300 ms). Then a go signal appeared, after which the participant had to press button 1 (meaningful) or 2 (meaningless) using the right hand. Finally, a blank screen was presented for a random time interval (1000 ± 300 ms). Then the next trial started. The assignment of response buttons was counterbalanced across participants. In the categorization task, hand (all meaningful) or face pictures were presented in random order. The participants were asked to discriminate face and hand, and to press button 1 or 2. The other conditions (trial timing, imperative stimulus, etc.) were the same as in the meaning task.

MEG recordings

Magnetic responses were measured using a 148-channel whole-head system (WHS2500, 4D-Neuroimaging, San Diego, CA, USA). Vertical and horizontal EOG were recorded simultaneously. Signals were recorded with a bandwidth of 0.1–100 Hz and digitized using a sample rate of 508.6 Hz. The continuous MEG data were filtered off-line with a 0.5- to 30-Hz band-pass filter. In each session, about 400 epochs were collected and averaged in a time window between −100 ms and +700 ms relative to stimulus onset. Epochs with motion or eye movement artifacts (more than 30 μV in horizontal or 50 μV in vertical eye movements), or with incorrect responses were excluded from averaging. If a subject had

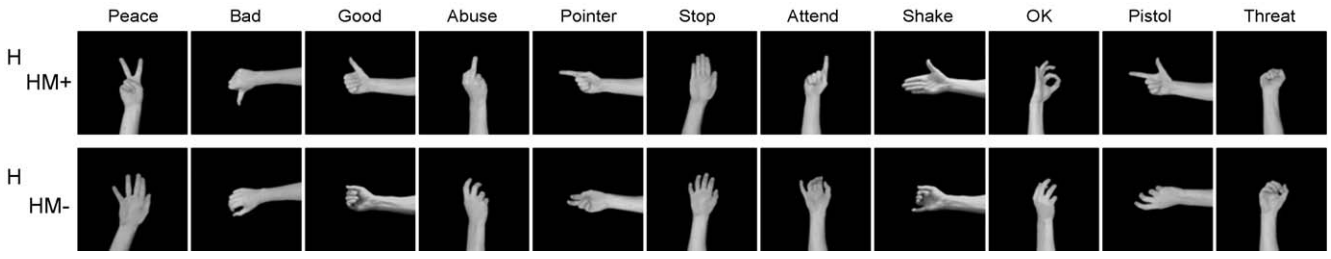

Fig. 1. All 11 meaningful hand signs (HM+) and their meaningless counterparts (HM−).

Table 1
Behavioral data

Meaning task (meaningful (HM+)/meaningless (HM−) hands discrimination)

Signs	Rating score		Performance (%)		Reaction time (ms)	
	HM+	HM−	HM+	HM−	HM+	HM−
Peace	4.91	1.70	95.1	81.8	587.3	617.0
Bad	4.87	1.89	95.5	95.1	591.4	619.6
Good	4.81	1.91	93.1	95.5	536.8	606.2
Abuse	4.62	2.00	88.7	91.5	580.6	603.4
Pointer	4.46	1.83	91.9	96.8	566.4	576.3
Stop	4.38	1.85	77.7	85.8	592.6	585.4
Attend	4.36	1.72	92.3	89.5	572.2	562.5
Shake	4.32	1.81	83.8	95.1	542.7	565.3
Ok	4.23	1.89	93.1	94.7	615.2	562.4
Pistol	4.20	1.56	94.7	95.5	556.7	576.1
Threat	4.19	1.91	72.1	91.9	612.8	613.4
Average (±SD)	4.49	1.82	88.9 ± 11.3	92.1 ± 5.5	576.4[a,b] ± 38.1	589.5[b] ± 33.1

Categorization task (hands (HC)/face (FC) categorization)

	Performance (%)		Reaction time (ms)	
	HC	FC	HC	FC
Average (±SD)	96.3 ± 3.5	97.1 ± 3.5	412.5[a,c] ± 33.1	409.6[c] ± 41.9

Rating score for each hand posture in psychological questionnaire (see Methods), performances during MEG measurements and reaction times for the meaning task (upper). Performances during MEG measurements and reaction times for the categorization task (lower). Superscripts a, b and c indicate the comparisons of the reaction times: HM+ with HC (a), HM+ with HM− (b) and HC with FC (c), respectively.
[a] $P < 0.000001$.

less than 70% correct responses to a hand sign, all epochs for that hand sign and also to its counterpart (meaningless hand sign) were excluded from the averaging process.

Spatially normalized current source density map

For each subject, a realistically shaped volume conductor was constructed from their individual MRI using ASA (ANT Software BV, Enschede, Netherlands). A reconstruction surface, at a depth of 1 cm below the brain envelope, was also created for each subject. Current source density (CSD) maps on the reconstruction surface were calculated individually. The CSD method is a minimum-norm least-squares (MNLS) algorithm as originally published by Hämäläinen and Ilmoniemi (1984, 1994). However, because this method tends to favor currents that have a high impact on the sensors, lead field normalization (Fuchs et al., 1999; Knösche et al., 1996) was applied, such that each weighted lead field column has the same Euclidian norm. The linear inverse was regularized using Tikhonov regularization. The regularization factor was computed according to the estimated signal-to-noise ratio (Knösche, 1997). The reconstruction surface was triangulated and at each of the 1222 nodes, two orthogonal tangential dipoles were placed, the strengths of which were then computed by the MNLS method. Finally, the two dipoles at one reconstruction node were combined into one. By this procedure, all brain activity was projected onto this surface. Then, each individual MRI was spatially normalized onto Talairach and Tournoux (1988) standard brain space by linear transformation. Each subject's CSD data were also spatially normalized using the identical transformation parameters.

PCA and PCA-based ROI analysis

A spatial PCA (Dien, 1998; Maess et al., 2002) was applied using the SAS software package (SAS Institute Inc., North Carolina, USA) as follows. At first, a rectangular matrix **A** was constructed that had a column for each CSD node (1222 columns). Within a column, time courses (−100 to +660 ms, 379 values) of all three conditions (HM+, HM− and HC) by 13 subjects were stored resulting in 14,781 (379 × 3 × 13) values per column. The principal components of the covariance matrix $\mathbf{A}^T\mathbf{A}$ of the matrix **A** were then calculated. The number of factors was determined according to their temporal profiles (time-locked with stimulus onset) and spatial profiles (anatomically and physiologically plausible distributions). After estimation of the factor number, the matrix of eigenvalues was truncated and the remaining subspace rotated using varimax rotation.

ROI analysis was based on the factors extracted from the PCA. We analyzed factors showing a PCA factor score greater than 0.01. Regions of interest were visually selected according to the magnitudes of the PCA factors, so that they included the areas with higher magnitudes shaping anatomically plausible subdivisions. In each ROI, time courses for the three conditions in CSD were calculated individually using an integrated time window of 10 ms. Condition effects were tested using two-way ANOVAs (Time and Condition) in each ROI with Bonferroni correction (divided by the number of the ROIs). Post hoc analyses were performed at all time windows that showed activity peaks using a paired t test with Bonferroni correction (divided by the number of condition contrasts tested). Individual activity was also analyzed at each of the ROIs. We regarded the CSD activity as being significant when a subject's activity was more than 3 SD (uncorrected $P < 0.001$) from the averaged baseline in time of interest 30 ms around the estimated peak latencies (Fig. 3, indicated by arrows).

Spatial accuracy of source estimation

In this study, we calculated CSD on a two-dimensional (2D) source space to obtain a reasonably stable solution with few assumptions. However, depth information is sacrificed in 2D estimation because all estimated currents are projected onto the reconstruction surface. As MEG is most sensitive to electrical sources located on the sulcal walls of the cortex (Hämäläinen et al., 1993; Hillebrand and Barnes, 2002), we chose a layer 1cm below the cortical envelope for the source space.

To test the spatial accuracy and validity of our 2D source estimation, we performed a simulation study using artificial dipoles as follows. First, we put artificial dipoles with all possible three orthogonal orientations at a specific cortical region in the standardized brain. Next, for each of these dipoles, magnetic fields at 148 channel positions were estimated by forward calculation using a realistic-shaped volume conductor. Then, we added Gausian random field noise to the magnetic fields with a variance of 1/15 of the signal variance. Finally, CSD was calculated from the estimated magnetic field data in the same manner as described above. Two simulation series were conducted. The first simulation series tested the reliability of the CSD solution on the 2D reconstruction surface using all ROI positions listed in Table 2. Additionally, we placed dipoles at

Table 2
Detailed information for ROIs determined by PCA shown in Fig. 3

Region		Brodmann's area	Individual activation	Talairach coordinates	ANOVA condition effects	PCA factor score
A	Primary visual	BA 17, 18	13	15, −85, 18	N.S.	0.052
B	Inferior occipitotemporal	BA 37, 19	11	−18, −67, −24* (Lt)	N.S.	0.364
		BA 37, 19		20, −40, −27* (Rt)		
C	Lt inferior temporal	BA 20, 21	11	−46, −7, −24	N.S.	0.029
D	Rt inferior temporal	BA 20, 21	11	41, −9, −27	$P < 0.0005$	0.030
E-p	Lt inferior parietal	BA 40	12	−47, −41, 35	N.S.	0.050
E-t	Lt STS	BA 22, 21	13	−48, −54, 11	$P < 0.001$	
F-p	Rt inferior parietal	BA 40, 2	13	53, −25, 27	$P < 0.05$	0.036
F-t	Rt STS	BA 22, 21	13	54, −38, −2	$P < 0.00001$	
G-t	Rt middle STS	BA 21	13	54, −17, −7	$P < 0.00001$	0.010
G-f	Rt fusiform	BA 37, 19	10	33, 4, −30 (ant)	$P < 0.01$	
				37, −47, −31* (post)		
H	Rt inferior frontal	BA 44, 45, 6	13	46, 14, 22	N.S.	0.016
I	Sensory-motor	BA 4, 3, 6, 2	13	−31, −6, 50 (Lt)	N.S.	0.100
				31, −27, 50 (Rt)		
J	Rt inferior prefrontal	BA 10, 11	12	30, 41, −6	$P < 0.0005$	0.030

The brain region, Brodmann's areas, number of subjects who showed significant activation in each ROI in the 13 subjects (Individual activation), coordinates of the center of gravity at each ROI in Talairach's brain (Talairach coordinates), statistical test for condition differences (ANOVA, after Bonferroni correction) and PCA factor score in each ROI corresponding to Fig. 3. The PCA factor score indicates explained variance of each PCA factors. Note that coordinate values in the inferior occipitotemporal ROI [B and G-f (post], indicated by asterisks) do not represent real values (see Spatial accuracy of source estimation section).

the medial part of the basal brain, which are included in PCA factors C and D (Fig. 3, PCA). Then, we calculated distances between the artificial dipole and the strongest extremum of the CSD contour. The second simulation series tested the possible biases in data interpretation. We simulated sources in other brain structures, which are not included in the reconstruction surface. With reference to the standard brain atlas (Talairach and Tournoux, 1988), we put artificial sources at the anterior, middle and posterior parts of the insula, cingulate cortex, hippocampus and inferior occipitotemporal regions. We analyzed whether these sources could create similar field distribution patterns on the reconstruction surface as those shown in the first simulation or not.

The results of the first simulation showed that if a source is located close to the reconstruction surface, the source estimation is reliable except the very medial part of the basal brain. The estimation errors (distance between artificial dipole and the extremum of simulated CSD) were less than 10 mm (5 mm on average) at all ROI positions listed in Table 2. At the medial part of the basal brain, the source estimation is less accurate with the estimation errors larger than 20 mm. Therefore, we did not interpret ROIs that included the medial part of PCA factors C and D (Fig. 3, PCA) in this study. The second simulation series suggested that there are two cases in which we should consider the effects of projection from deeper sources to the reconstruction surface. (1) A potential source in the most anterior part of the insula can create the similar CSD pattern as a source in the inferior frontal cortex. This suggests that the electric activity in ROI H can be explained by sources either in the inferior frontal cortex or insula. (2) The brain envelope used for the source space in this study includes the cerebellum, which covers the posterior part of the basal brain. We found that bilateral potential sources, either in the cerebellum or in the occipitotemporal regions, can create similar CSD patterns in ROI B (Fig. 3). However, we would expect ROI B to reflect activity from inferior occipitotemporal regions. Since MEG detects the postsynaptic potentials in the apical dendrites of the pyramidal neurons (Hämäläinen et al., 1993), the cerebellum is theoretically less capable of producing strong magnetic fields compared to the cerebral cortex.

Results

Behavioral performances

Behavioral performances associated with the two tasks are presented in Table 1. No significant condition differences in the reaction performances during MEG measurements between HM+ and HM−, and between HC and FC were found. The mean reaction time for the HM+ condition (576.4 ms) was significantly longer than that for the HC condition (412.5 ms).

MEG data

Fig. 2 shows CSD maps of the HM+ condition (HM+) and their condition contrasts with HM− (HM+ vs. HM−) and with HC (HM+ vs. HC), averaged across 13 subjects on spatially normalized space. Electric activation began at the occipital pole and then spread ventrally through occipitotemporal regions, and also dorsally through occipito-parieto-frontal regions. The right hemisphere generally showed stronger electric activation than the left (Fig. 2, HM+). Condition subtractions showed that HM+ elicited stronger activity than both HM− and HC in the right parietal and temporal regions, in the latencies around 210 and 390ms (Fig. 2, HM+ vs. HM− and HM+ vs. HC). In contrast, HC elicited stronger activity than HM+ in the left occipito-parieto-temporal regions in the latencies around 210 and 330 ms (Fig. 2, HM+ vs. HC).

PCA extracted 10 factors, which account for 72.3% of the total variance, from the CSD data of three conditions (HM+, HM− and HC) (Fig. 3, PCA). We created 13 ROIs from these 10 PCA factors (Fig. 3, ROI, Table 2). Averaged time courses of CSD in the three conditions at each ROI are shown in the right column (Time course) of Fig. 3. Ten of the thirteen subjects

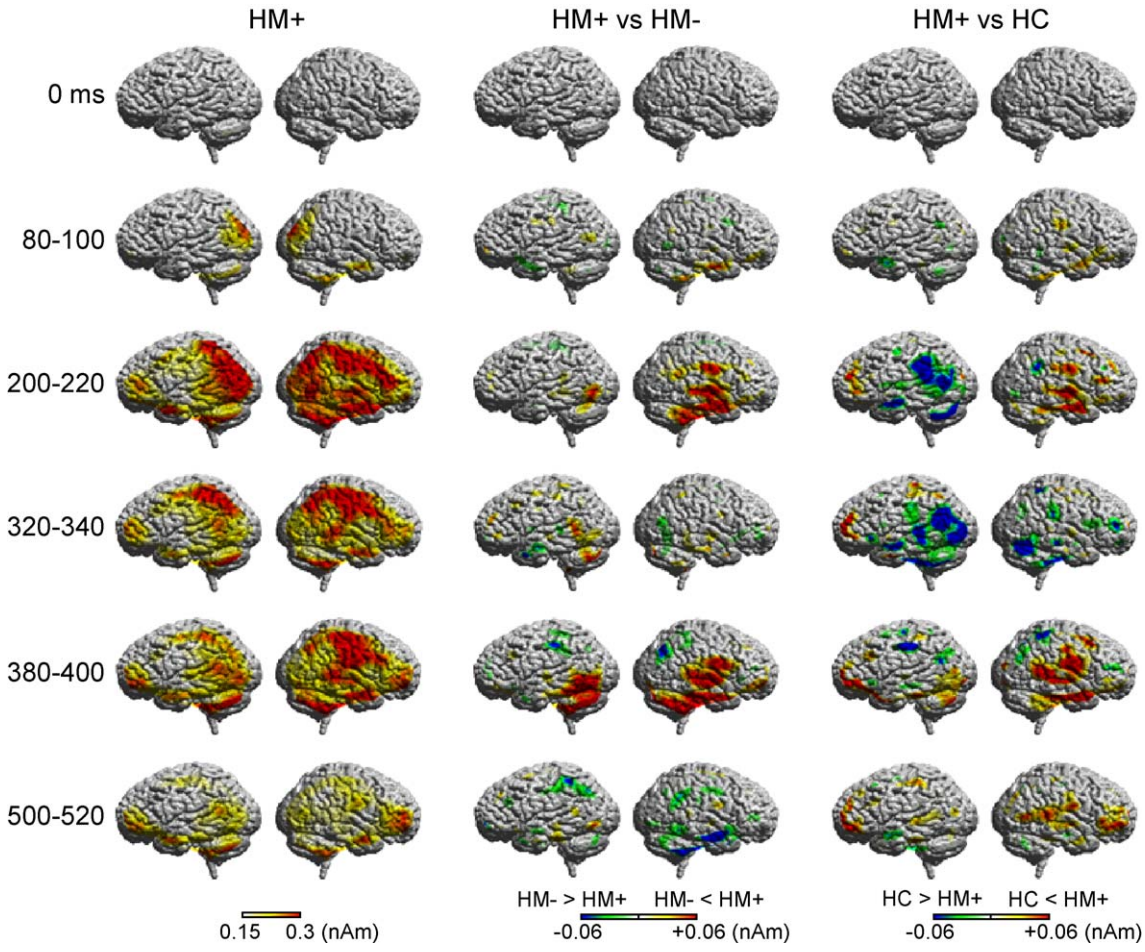

Fig. 2. Spatially normalized CSD maps and their condition contrasts. Each two columns show CSD in the HM+ condition (left), condition subtraction between HM+ and HM− (middle), and between HM+ and HC (right). Each row indicates time windows in which the CSD was calculated.

showed significant activation in all 13 ROIs, and all 13 subjects showed significant activation in a subset of seven ROIs (A, E-t, F-p, F-t, G-t, H and I) (Table 2). Each ROI showed characteristic time courses in averaged regional electrical activity (Fig. 3, Time course). ROI A displayed monophasic time courses, which peaked in the latency around 120 ms. ROIs B, C, D and G-f showed the first activity peaking at around 170 ms. Moreover, both ROIs D and G-f had two additional peaks around 230 and 380 ms in the HM condition. E-p and E-t showed biphasic activity, which were most prominent in the HC condition. Both pairs of peaks in E-p and E-t were around 200 and 340 ms, and 180 and 330 ms, respectively. F-p, F-t, G-t and H displayed similar biphasic time courses in the HM+ condition, with a pair of peaks around 230 and 370 ms. ROI I showed a large peak around 340 ms with a smaller peak around 200 ms. ROI J showed sustained activity from 150 ms, which lasted until the end of the analyzed time window except the HC condition.

Significant condition effects in time courses were found in 7 of 13 ROIs (Table 2, ANOVA condition effects, Fig. 3). Post hoc analyses also detected significant condition differences in seven ROIs at their peak activation latencies (Fig. 3). Significant activation in HM+ compared with HM− was found in ROIs D, F-p, F-t, G-t and G-f. Moreover, ROIs D, F-p and F-t also showed significantly stronger activity in HM+ than HC. Those five ROIs showed similar activation patterns having two peaks around 230 and 370–380 ms. ROI E-t showed significant activation in HC compared with HM+ (Fig. 3).

Discussion

Involvement of multiple neuronal systems in hand sign recognition

The CSD maps showed widely distributed electrical activity, which spread to occipital, temporal, parietal and frontal lobes, following hand sign presentation (Fig. 2). The application of the PCA appeared to successfully extract spatiotemporally separable electrical activity from the CSD data because each PCA factor showed a physiologically plausible distribution (Fig. 3, PCA). There were at least 10 independent factors, which contained anatomically distinct subdivisions (Fig. 3, ROI, Table 2), involved in hand sign recognition. We consider that most of these multiple brain regional activation can be explained by processing within the following four neuronal systems: (1) *Primary visual system*. The effects in ROI A should mainly reflect the activation of the primary visual cortices. The time courses of the effects, which indicated increased activity around 50 ms with a peak at about 120 ms after stimulus onset, are compatible with previous electrophysiological studies (Nakamura et al., 1997; Yoneda et al., 1995). (2) *Object recognition system*. Ventral occipitotemporal

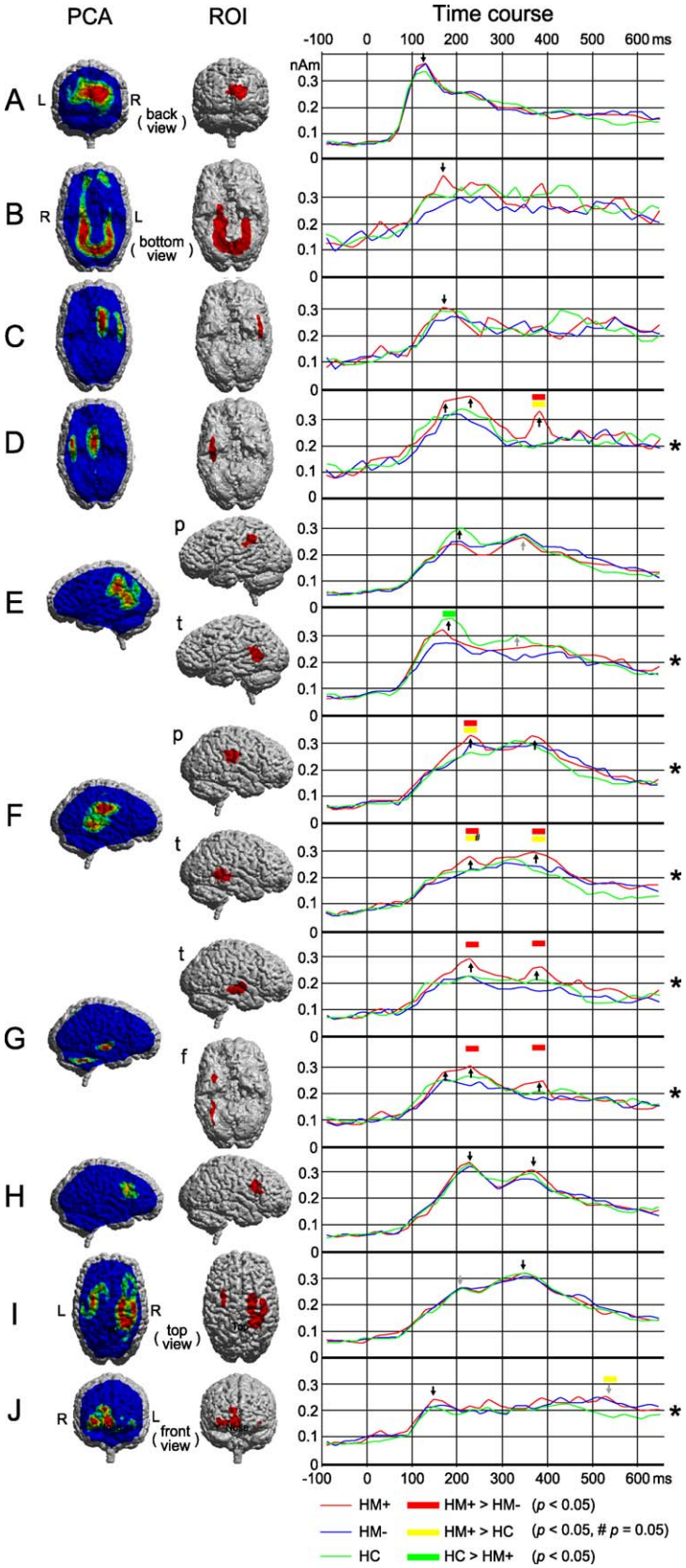
PCA
ROI
Time course
-100 0 100 200 300 400 500 600 ms
nAm
0.3
0.2
0.1
0
A
L
R
(back view)
B
R
L
(bottom view)
C
D
p
E
t
F
p
t
G
t
f
H
I
L
R
(top view)
J
R
L
(front view)
*
-100 0 100 200 300 400 500 600 ms
HM+
HM-
HC
HM+ > HM- (p < 0.05)
HM+ > HC (p < 0.05, # p = 0.05)
HC > HM+ (p < 0.05)

regions, including the fusiform face area and inferior temporal cortex, are known to process different categories of objects as well as faces (Gerlach et al., 1999; Haxby et al., 2001; Sergent et al., 1992; Ungerleider and Haxby, 1994). Therefore, activation within ROIs B, C, D and G-f were considered to reflect processing in the object recognition system. The latencies of their first peak in activity at around 170 ms are also compatible with studies for face and object recognition (Allison et al., 1994; Botzel et al., 1995; Ioannides et al., 2000; Nakamura et al., 2001; Sams et al., 1997; Tanaka and Curran, 2001). (3) *Mirror neuron system*. Activation within the inferior frontal (ROI H) (see Spatial accuracy of source estimation section), inferior parietal (ROIs E-p and F-p) and STS (ROIs E-t, F-t and G-t) regions can be explained by the mirror neuron system (see Introduction). Although the stimuli we used were static images, the activation of the mirror neuron system seems plausible. Several studies have shown that static images of body parts that imply motion activate identical brain areas as dynamic images (Allison et al., 2000; Kourtzi and Kanwisher, 2000; Nishitani and Hari, 2002; Senior et al., 2000). Activation observed in the sensory-motor cortices (ROI I) could also be related to the mirror neuron system because the observation of hands is known to activate the motor cortex as a result of mirror neuron excitation (Hari et al., 1998; Nishitani and Hari, 2000). Note that these activity profiles are not the results of motor reactions, as the tasks demanded delayed responses, and all subjects used only their *right* hands to respond. (4) *Social recognition system*. The concept of the social recognition system (Adolphs, 1999) can also account for the activation in the STS (ROIs E-t, F-t and G-t), inferior prefrontal (ROI J) and sensory-motor (ROI I) regions. The STS is part of both the mirror neuron and the social recognition systems (see Introduction). The importance of the ventromedial prefrontal cortex in social recognition has been demonstrated in lesion (Stone et al., 1998), functional imaging (Cavada and Schultz, 2000) and electrophysiological studies (Kawasaki et al., 2001). The right somatosensory cortex is considered to contribute to the recognition of social signals (Adolphs, 1999) because lesions in the right somatosensory cortices cause impaired ability to assess other people's emotional states (Adolphs et al., 1996). Although it is difficult to distinguish between pre- and postcentral activation with our methods, the shape (larger in the right than the left) and the coordinates (2 cm more posterior in the right than the left) of ROI I (Fig. 3 and Table 2) suggest involvement of the right primary somatosensory cortex in hand sign recognition. This is consistent with the involvement of the somatosensory cortices during observation of hand actions (Avikainen et al., 2002; Rossi et al., 2002). It is known that the amygdala also plays an important role in social recognition (Adolphs, 1999; Kawashima et al., 1999; Oya et al., 2002). The medial part of the PCA factor C and D (Fig. 3) might partially represent activity from the amygdala or parahippocampal structure. However, we did not analyze these activities in this study due to the spatial accuracy problems in our method highlighted in the simulation studies (see Spatial accuracy of source estimation section).

Brain regions responsible for interpreting the meaning of hand signs

We consider that brain regions showing significant activation in the HM+ condition as compared with HM− should be associated with the cognitive stages for assessing the meaning of the hand signs. This is based on the assumptions that (1) there should be stored memory representations for meaningful hand signs, and (2) if a task demands access to memory, neuronal populations associated with memory templates should be activated. Such neuronal properties were found in the right inferior occipitotemporal (Figs. 3D and G-f), right inferior parietal (Fig. 3, F-p) and right STS (Figs. 3F-t and G-t) regions. These brain areas belong to the object recognition, mirror neuron and social recognition systems, respectively. The activity in the right inferior temporal, inferior parietal and STS regions also showed task-dependent effects. The activation due to meaningful hand postures during the meaning task (HM+) was significantly stronger than that during the categorization task (HC) (Figs. 3D, F-p and F-t), although the stimulus sets of the two conditions were identical. We consider this result a top-down effect relevant for the recognition of hand signs.

Cooperation across the different neuronal systems

The regional electric activation associated with processing hand sign meanings showed interesting temporal profiles. All of the five regions (D, F-p, F-t, G-t and G-f) showed similar time courses in the HM+ condition in a time window from 200 to 400 ms, with two peaks in activity around 230 and 370–380 ms (Fig. 3). Especially, there is close similarity in the entire time courses between F-p and F-t, and also between G-t and G-f, because each of the pairs belonged to one PCA factor (Figs. 3F and G, respectively). It is important to consider whether these observations reflect true correlated activity from different brain regions, or are pseudo-phenomena affected by neighboring source activity (cross-talk effect) (Fujimaki et al., 2002) and/or blurring of the current sources. We argue that most of these effects represent real correlated-activity for the following reasons: (1) Each of the PCA factors, especially those which included separate brain regions (e.g. Figs. 3B, E, F, G and I), showed physiologically plausible spatial distributions. These distributions cannot be explained by the influence of neighboring sources nor blurring. (2) These findings are supported by previous anatomical research showing that the STS neurons are connected with neurons both in the inferior parietal and inferior temporal cortices (Oram and Perrett, 1996; Rizzolatti and Luppino, 2001). Therefore, it is reasonable to assume that there should exist communication between different neuronal systems, and that distinct brain regions, including the inferior parietal, STS and inferior occipitotemporal cortices, harmoniously work together during hand sign recognition.

Fig. 3. Spatial distribution of each factor extracted by PCA (column PCA), ROI patterns created from PCA (ROI) and time courses of CSD averaged across the 13 subjects in each ROI (Time course). Viewpoints of the brains are from the back (row A), from the bottom (B–D, G-f), from the left (E), from the right (F, G-t, H), from the top (I) and from the front (J). Time courses of the three conditions are plotted with red (HM+), blue (HM−) and green (HC). Time courses, which showed statistical significant condition differences ($P < 0.05$, ANOVA after Bonferroni correction), are indicated by asterisks (see Table 2). Time windows, during which statistically significant condition differences occurred ($P < 0.05$), are indicated in red (HM+ > HM−), yellow (HM+ > HC) and green (HC > HM+) bars. ROIs, which include medial part of the PCA factors C and D, are not analyzed (see Methods). Both black and gray arrows indicate estimated peak latencies. Latencies indicated by black arrows were discussed in detail (see Discussion and Fig. 4).

Oram and Perrett (1996) have suggested that information from both ventral and dorsal pathways should be integrated through the STS. Such integration processes might play an important role in solving the binding problem.

Interhemispheric differences in hand sign processing

One of the most striking results was the marked hemispheric asymmetry, in that most of the regions associated with processing the meaningful hand signs were in the right hemisphere. By contrast, in the studies investigating action perception, meaningful actions mainly activated regions in the left hemisphere (Decety et al., 1997; Grafton et al., 1996; Rizzolatti et al., 1996b). Decety and Grezes (1999) considered that the left hemispheric predominance in meaningful action perception could be interpreted as the activation of semantic representations related to language, a conclusion that is consistent with the left-hemispheric specialization for language and motor control. On the other hand, the right hemispheric predominance has been suggested by the literature on emotional and social recognition (Adolphs, 1999; Adolphs et al., 1996; Happe et al., 1999; Nakamura et al., 1999). Similar to facial expression (Adolphs et al., 1996; Nakamura et al., 1999), "hand expression" appears to be processed predominantly in the right hemisphere as one type of social signal.

Roles of the left parietotemporal regions

Activation of the parietotemporal regions was also found in the left hemisphere (Figs. 3E-p and E-t). The largest effects in these regions were elicited by the HC condition and peaked around 180–200 ms, whereas the right counterparts, which peaked about 40 ms later, reacted strongest to the HM+ condition. The earlier activation in the left hemisphere compared with the right suggests that the left regions have a more primary role for visuo-somatic analysis of hand postures. This concept is consistent with various patient studies, showing that lesions involving the parietotemporal regions in the dominant hemisphere cause several types of apraxia (Leiguarda and Marsden, 2000). The strongest activation in the HC condition suggests that the left parietotemporal regions also have an important function associated with hand categorization.

A spatiotemporal structure of information processes in hand sign recognition

The present study enabled us to depict global aspects of information processing in the spatiotemporal domain during hand sign recognition. Fig. 4 shows our hand sign recognition model consists of processes in four neuronal systems. After the primary

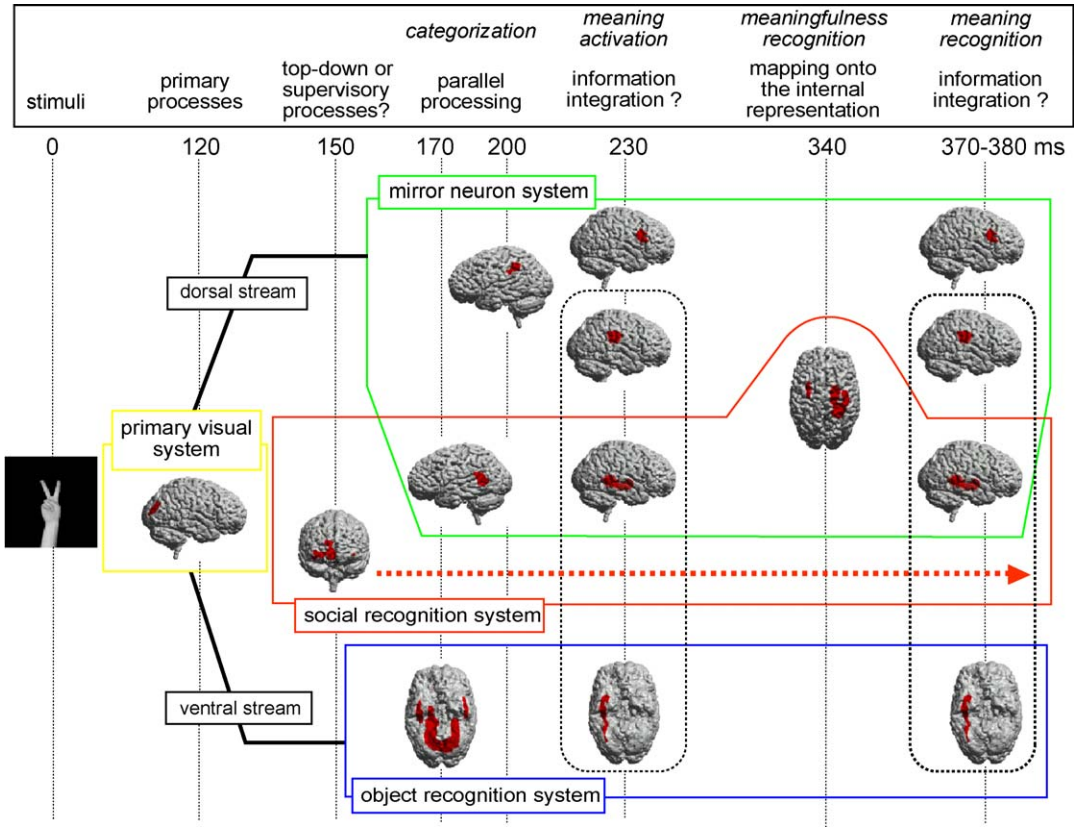

Fig. 4. Schematic presentation of possible brain mechanisms used to recognize hand signs. Brain pictures with ROIs are grouped into four neuronal systems: the primary visual (color coded in yellow), mirror neuron (green), social recognition (orange) and object recognition (blue) systems. They are arranged horizontally according to the peak latencies in ROI activation. Latencies of interest were determined from estimated peak latencies in Fig. 3 (indicated by black arrows). Brain regions, which showed similar condition effects and time courses, are surrounded by black dotted lines. Note that ROIs, which belong to the same anatomical subdivisions and also showed similar time courses, are projected onto one brain picture; for example, both ROIs in the STS (F-t and G-t in Fig. 3) are projected onto one brain picture (social recognition system, 230 and 370–380 ms). Similarly, ROIs B, C, D and G-f (object recognition system, 170 ms), and ROIs D and G-f (object recognition system, 230 and 370–380 ms) are also combined.

visual processes peaking around 120 ms, different aspects of information are processed in parallel in anatomically distinct brain areas. The first peak activation of these parallel processes occur at about 170–200 ms. Thereafter, distinct brain areas are simultaneously activated suggesting cooperation across different neuronal systems (230 ms). At around 340 ms, the somatomotor cortices are maximally active. Finally, the different brain regions are again activated in concert (370–380 ms). The right inferior prefrontal region showed interesting time courses (Fig. 3J), in that it is activated quite early (150 ms), and continuously active through the task except in the HC condition (indicated by broken orange line). This time course suggests that the right inferior prefrontal cortex might have a function associated with top-down and/or supervisory (monitoring) processes throughout the entire process of hand sign recognition.

We estimated the timing of the cognitive events by combining MEG data with the behavioral results from the reaction time study. It took about 160 ms longer to judge meaningful or meaningless hands than to judge hands or faces (Table 1). If we assume the timing of categorization to be around 180 ms, during which HC showed the largest condition effect (Fig. 3E), the time required to recognize the meaningfulness of hand signs should be around 340 ms (180 + 160 ms = 340 ms). This estimate is consistent with the ''simulation theory'' that we understand other individual's mind by representing his/her state in our own brain. It is postulated that an actor's intention is understood when the observed action is mapped onto our motor representations (Decety and Grezes, 1999). Analogously, it is also proposed that we infer another person's emotional and social status from the facial expression by generating somatosensory images internally (Adolphs, 1999). Therefore, it appears to be plausible that the effects with latencies of around 340 ms, during which the somatomotor cortices showed activity peaks, might be associated with recognizing the ''meaningfulness'' of hand signs. We also speculate that the concrete ''meaning'' of each hand sign can be recognized within about 380 ms for the following reasons. There were two activation peaks in HM+ with significant condition effects, which perhaps reflect processes associated with the interpretation of meaning (230 and 370–380 ms). The two processing stages appeared to be comparable with two stages of processing analogously proposed for word recognitions (Marslen-Wilson, 1987): the first peak might correspond to meaning activation (lexical access) and the second might correspond to meaning selection (recognition).

Acknowledgments

We are grateful to J. Haxby, S. Pollmann, M. Blass, A. Anwander, P. Sivonen, S. Rueschemeyer, G. Barnes, T. Penney, T. Kato and S. Kawatsu for helpful comments, and to Y. Wolff for technical assistance.

References

Adolphs, R., 1999. Social cognition and the human brain. Trends Cogn. Sci. 3, 469–479.

Adolphs, R., Damasio, H., Tranel, D., Damasio, A.R., 1996. Cortical systems for the recognition of emotion in facial expressions. J. Neurosci. 16, 7678–7687.

Allison, T., Ginter, H., McCarthy, G., Nobre, A.C., Puce, A., Luby, M., Spencer, D.D., 1994. Face recognition in human extrastriate cortex. J. Neurophysiol. 71, 821–825.

Allison, T., Puce, A., McCarthy, G., 2000. Social perception from visual cues: role of the STS region. Trends Cogn. Sci. 4, 267–278.

Avikainen, S., Forss, N., Hari, R., 2002. Modulated activation of the human SI and SII cortices during observation of hand actions. NeuroImage 15, 640–646.

Botzel, K., Schulze, S., Stodieck, S.R., 1995. Scalp topography and analysis of intracranial sources of face-evoked potentials. Exp. Brain Res. 104, 135–143.

Calvert, G.A., Bullmore, E.T., Brammer, M.J., Campbell, R., Williams, S.C.R., McGuire, P.K., Woodruff, P.W.R., Iverson, S.D., David, A.S., 1997. Activation of auditory cortex during silent lipreading. Science 276, 593–596.

Carruthers, P., Smith, P.K. (Eds.), 1996. Theories of Theories of Mind. Cambridge Univ. Press, Cambridge, UK.

Cavada, C., Schultz, W., 2000. The mysterious orbitofrontal cortex. Foreword. Cereb. Cortex 10, 205.

Decety, J., Grezes, J., 1999. Neural mechanisms subserving the perception of human actions. Trends Cogn. Sci. 3, 172–178.

Decety, J., Grezes, J., Costes, N., Perani, D., Jeannerod, M., Procyk, E., Grassi, F., Fazio, F., 1997. Brain activity during observation of actions-Influence of action content and subject's strategy. Brain 120, 1763–1777.

Dien, J., 1998. Addressing misallocation of variance in principal components analysis of event-related potentials. Brain Topogr. 11, 43–55.

Fogassi, L., Gallese, V., Fadiga, L., Rizzolatti, G., 1998. Neurons responding to the sight of goal directed hand/arm actions in the parietal area PF (7b of the macaque monkey. Abstr. - Soc. Neurosci. 24, 257.

Fuchs, M., Wagner, M., Kohler, T., Wischmann, H.A., 1999. Linear and nonlinear current density reconstructions. J. Clin. Neurophysiol. 16, 267–295.

Fujimaki, N., Hayakawa, T., Nielsen, M., Knösche, T.R., Miyauchi, S., 2002. An fMRI-Constrained MEG source analysis with procedures for dividing and grouping activation. NeuroImage 17, 324–343.

Gerlach, C., Law, I., Gade, A., Paulson, O.B., 1999. Perceptual differentiation and category effects in normal object recognition—A PET study. Brain 122, 2159–2170.

Goldin-Meadow, S., 1999. The role of gesture in communication and thinking. Trends Cogn. Sci. 3, 419–429.

Grafton, S.T., Arbib, M.A., Fadiga, L., Rizzolatti, G., 1996. Localization of grasp representations in humans by positron emission tomography. 2. Observation compared with imagination. Exp. Brain Res. 112, 103–111.

Grossman, E., Donnelly, M., Price, R., Pickens, D., Morgan, V., Neighbor, G., Blake, R., 2000. Brain areas involved in perception of biological motion. J. Cogn. Neurosci. 12, 711–720.

Hämäläinen, M., Ilmoniemi, R.J., 1984. Interpreting measured magnetic fields of the brain: estimates of current distributions. Technical Report TKK-F-A559, Helsinki University of Technology, Helsinki.

Hämäläinen, M.S., Ilmoniemi, R.J., 1994. Interpreting magnetic—Fields of the brain—Minimum norm estimates. Med. Biol. Eng. Comput. 32, 35–42.

Hämäläinen, M., Hari, R., Ilmoniemi, R.J., Knuutila, J., Lounasmaa, O.V., 1993. Magnetoencephalography. Rev. Mod. Phys. 65, 413–496.

Happe, F., Brownell, H., Winner, E., 1999. Acquired 'theory of mind' impairments following stroke. Cognition 70, 211–240.

Hari, R., Forss, N., Avikainen, S., Kirveskari, E., Salenius, S., Rizzolatti, G., 1998. Activation of human primary motor cortex during action observation: a neuromagnetic study. Proc. Natl. Acad. Sci. U. S. A. 95, 15061–15065.

Haxby, J.V., Gobbini, M.I., Furey, M.L., Ishai, A., Schouten, J.L., Pietrini, P., 2001. Distributed and overlapping representations of faces and objects in ventral temporal cortex. Science 293, 2425–2430.

Hillebrand, A., Barnes, G.R., 2002. A quantitative assessment of the sensitivity of whole-head MEG to activity in the adult human cortex. NeuroImage 16, 638–650.

Iacoboni, M., Woods, R.P., Brass, M., Bekkering, H., Mazziotta, J.C., Rizzolatti, G., 1999. Cortical mechanisms of human imitation. Science 286, 2526–2528.

Iacoboni, M., Koski, L.M., Brass, M., Bekkering, H., Woods, R.P., Dubeau, M.C., Mazziotta, J.C., Rizzolatti, G., 2001. Reafferent copies of imitated actions in the right superior temporal cortex. Proc. Natl. Acad. Sci. 98, 13995–13999.

Ioannides, A.A., Liu, L.C., Kwapien, J., Drozdz, S., Streit, M., 2000. Coupling of regional activations in a human brain during an object and face affect recognition task. Hum. Brain Mapp. 11, 77–92.

Kawasaki, H., Adolphs, R., Kaufman, O., Damasio, H., Damasio, A.R., Granner, M., Bakken, H., Hori, T., Howard, M.A., 2001. Single-neuron responses to emotional visual stimuli recorded in human ventral prefrontal cortex. Nat. Neurosci. 4, 15–16.

Kawashima, R., Sugiura, M., Kato, T., Nakamura, A., Hatano, K., Ito, K., Fukuda, H., Kojima, S., Nakamura, K., 1999. The human amygdala plays an important role in gaze monitoring—A PET study. Brain 122, 779–783.

Knösche, T.R., 1997. Solutions of the neuroelectromagnetic inverse problem—An evaluation study. PhD thesis, University of Twente, The Netherlands.

Knösche, T., Praamstra, P., Stegeman, D., Peters, M., 1996. Linear estimation discriminates midline sources and a motor cortex contribution to the readiness potential. Electroencephalogr. Clin. Neurophysiol. 99, 183–190.

Kourtzi, Z., Kanwisher, N., 2000. Activation in human MT/MST by static images with implied motion. J. Cogn. Neurosci. 12, 48–55.

Leiguarda, R.C., Marsden, C.D., 2000. Limb apraxias—Higher-order disorders of sensorimotor integration. Brain 123, 860–879.

Livingstone, M., Hubel, D., 1988. Segregation of form, color, movement, and depth-anatomy, physiology, and perception. Science 240, 740–749.

McNeill, D., 1992. Hand and Mind: What Gestures Reveal about Thought Univ. of Chicago Press, Chicago.

Maess, B., Friederici, A.D., Damian, M., Meyer, A.S., Levelt, W.J.M., 2002. Semantic category interference in overt picture naming: sharpening current density localization by PCA. J. Cogn. Neurosci. 14, 455–462.

MarslenWilson, W.D., 1987. Functional parallelism in spoken word-recognition. Cognition 25, 71–102.

Nakamura, A., Kakigi, R., Hoshiyama, M., Koyama, S., Kitamura, Y., Shimojo, M., 1997. Visual evoked cortical magnetic fields to pattern reversal stimulation. Cogn. Brain Res. 6, 9–22.

Nakamura, K., Kawashima, R., Ito, K., Sugiura, M., Kato, T., Nakamura, A., Hatano, K., Nagumo, S., Kubota, K., Fukuda, H., Kojima, S., 1999. Activation of the right inferior frontal cortex during assessment of facial emotion. J. Neurophysiol. 82, 1610–1614.

Nakamura, A., Yamada, T., Abe, Y., Nakamura, K., Sato, N., Horibe, K., Kato, T., Kachi, T., Ito, K., 2001. Age-related changes in brain neuromagnetic responses to face perception in humans. Neurosci. Lett. 312, 13–16.

Nishitani, N., Hari, R., 2000. Temporal dynamics of cortical representation for action. Proc. Natl. Acad. Sci. U. S. A. 97, 913–918.

Nishitani, N., Hari, R., 2002. Viewing lip forms: cortical dynamics. Neuron 36, 1211–1220.

Oram, M.W., Perrett, D.I., 1994. Responses of anterior superior temporal polysensory (STPA) neurons to biological motion stimuli. J. Cogn. Neurosci. 6, 99–116.

Oram, M.W., Perrett, D.I., 1996. Integration of form and motion in the anterior superior temporal polysensory area (STPa) of the macaque monkey. J. Neurophysiol. 76, 109–129.

Oya, H., Kawasaki, H., Howard, M.A., Adolphs, R., 2002. Electrophysiological responses in the human amygdala discriminate emotion categories of complex visual stimuli. J. Neurosci. 22, 9502–9512.

Perrett, D.I., Smith, P.A.J., Potter, D.D., Mistlin, A.J., Head, A.S., Milner, A.D., Jeeves, M.A., 1985. Visual cells in the temporal cortex sensitive to face view and gaze direction. Proc. R. Soc. Lond., Ser. B Biol. Sci. 223, 293–317.

Perrett, D.I., Harries, M.H., Bevan, R., Thomas, S., Benson, P.J., Mistlin, A.J., Chitty, A.J., Hietanen, J.K., Ortega, J.E., 1989. Frameworks of analysis for the neural representation of animate objects and actions. J. Exp. Biol. 146, 87–113.

Puce, A., Allison, T., Bentin, S., Gore, J.C., McCarthy, G., 1998. Temporal cortex activation in humans viewing eye and mouth movements. J. Neurosci. 18, 2188–2199.

Rizzolatti, G., Luppino, G., 2001. The cortical motor system. Neuron 31, 889–901.

Rizzolatti, G., Fadiga, L., Gallese, V., Fogassi, L., 1996a. Premotor cortex and the recognition of motor actions. Cogn. Brain Res. 3, 131–141.

Rizzolatti, G., Fadiga, L., Matelli, M., Bettinardi, V., Paulesu, E., Perani, D., Fazio, F., 1996b. Localization of grasp representations in humans by PET. 1. Observation versus execution. Exp. Brain Res. 111, 246–252.

Rizzolatti, G., Fogassi, L., Gallese, V., 2001. Neurophysiological mechanisms underlying the understanding and imitation of action. Nat. Rev., Neurosci. 2, 661–670.

Rossi, S., Tecchio, F., Pasqualetti, P., Ulivelli, M., Pizzella, V., Romani, G.L., Passero, S., Battistini, N., Rossini, P.M., 2002. Somatosensory processing during movement observation in humans. Clin. Neurophysiol. 113, 16–24.

Sams, M., Hietanen, J.K., Hari, R., Ilmoniemi, R.J., Lounasmaa, O.V., 1997. Face-specific responses from the human inferior occipito-temporal cortex. Neuroscience 77, 49–55.

Senior, C., Barnes, J., Giampietro, V., Simmons, A., Bullmore, E.T., Brammer, M., David, A.S., 2000. The functional neuroanatomy of implicit-motion perception or 'representational momentum'. Curr. Biol. 10, 16–22.

Sergent, J., Ohta, S., Macdonald, B., 1992. Functional neuroanatomy of face and object processing—A positron emission tomography study. Brain 115, 15–36.

Stone, V.E., Baron-Cohen, S., Knight, R.T., 1998. Frontal lobe contributions to theory of mind. J. Cogn. Neurosci. 10, 640–656.

Talairach, J., Tournoux, P., 1988. Co-planar Stereotaxic Atlas of the Human Brain: 3-Dimentional Proportional System: An Approach to Cerebral Imaging Thime, Stuttgart.

Tanaka, J.W., Curran, T., 2001. A neural basis for expert object recognition. Psychol. Sci. 12, 43–47.

Ungerleider, L.G., Haxby, J.V., 1994. 'What' and 'where' in the human brain. Curr. Opin. Neurobiol. 4, 157–165.

Wicker, B., Michel, F., Henaff, M.A., Decety, J., 1998. Brain regions involved in the perception of gaze: a PET study. NeuroImage 8, 221–227.

Wolfe, J.M., Cave, K.R., 1999. The psychophysical evidence for a binding problem in human vision. Neuron 24, 11–17.

Yoneda, K., Sekimoto, S., Yumoto, M., Sugishita, M., 1995. The early component of the visual-evoked magnetic-field. NeuroReport 6, 797–800.